Journal of Nuclear Materials 433 (2013) 143–151

Contents lists available at SciVerse ScienceDirect

Journal of Nuclear Materials

journal homepage: www.elsevier.com/locate/jnucmat

# First principles calculations of the structure and elastic constants of α, β and γ uranium

Benjamin Beeler [a,*], Chaitanya Deo [a], Michael Baskes [b,c], Maria Okuniewski [d]

[a] Nuclear and Radiological Engineering Program, George W. Woodruff School of Mechanical Engineering, Georgia Institute of Technology, 770 State Street, Atlanta, GA 30332, USA
[b] University of California, San Diego, 9500 Gilman Drive, La Jolla, CA 92093, USA
[c] Los Alamos National Laboratory, PO Box 1663, Los Alamos, NM 87545, USA
[d] Idaho National Laboratory, PO Box 1625, Idaho Falls, ID 83415, USA

ARTICLE INFO

*Article history:*
Received 2 February 2012
Accepted 12 September 2012
Available online 23 September 2012

ABSTRACT

This study analyzes structural and elastic properties of five uranium crystal structures: the face centered orthorhombic A20 (α phase), the tetragonal D8$_b$ (β phase), body centered tetragonal (bct), body centered cubic (γ phase) and face centered cubic structures. Calculations are performed within the density functional theory framework employing the Projector Augmented Wave method and the Perdew–Burke–Ernzerhof generalized gradient approximation (PBE–GGA) of the exchange correlation. The elastic constants are used to compute polycrystalline elastic moduli, Poisson's ratio and the Debye temperature for all five structures. The α and γ phase properties are compared with theoretical and experimental results. The complex tetragonal 30 atom beta phase is examined in detail. Representation of the β phase by a bct structure is examined; we find that the structure of the β phase is significantly different from the bct phase but exhibits similar elastic properties. This is the first comprehensive investigation into the elastic constants of uranium utilizing the PBE–GGA.

## 1. Introduction

The metal uranium exists in three solid phases: α (face-centered orthorhombic), β (tetragonal) and γ (body-centered cubic). At elevated temperatures, uranium transforms from α to β [1] at approximately 935 K and β transforms to γ at approximately 1045 K [2]. The electronic structure of uranium is dominated by 5*f* electron states that form narrow bands that tend to bond the atoms in complex and distorted ways [3–5]. Electronic structure calculations have had varied success in describing these complex structures. Söderlind [4] calculated the structural and elastic properties of orthorhombic α-uranium using the full-potential linear muffin tin orbital technique. While the calculated lattice constants had an accuracy of approximately 1% compared to the experimental values (determined at 50 K) [6], the elastic constants were much more difficult to model and compare with experiment, partially because no internal relaxation was allowed during the finite distortion technique and also because uranium undergoes significant phonon softening as a function of temperature. The qualitative trends between the elastic constants were, however, in good agreement with the experimental values. The root-mean-square deviation of the elastic moduli, $c_{11}$ through $c_{66}$, was 118 GPa [7]. Söderlind also calculated the equilibrium lattice constant of body-centered cubic (bcc) γ uranium. These calculated values overestimate the experimental lattice constants at 0 K.

Although the full-potential calculations are able to capture the physics of the atomic and electronic interactions that dictate many of the properties of the orthorhombic uranium crystal, they are not yet of sufficient computational efficiency to allow the simulation of more complex systems (i.e., larger supercells containing crystal defects, such as vacancies, and/or impurity atoms). Also, the β phase of uranium has a complicated 30 atom unit cell. Using full-potential calculations to analyze such a large and complex unit cell can become untenable.

However, an earlier study by Crocombette et al. [8] using a norm-conserving pseudopotential, in which the core electrons are replaced by an effective electron–electron interaction potential allowing for the investigation of more complex systems, was not so accurate. For α uranium, the lattice constant for the b vector of the orthorhombic crystal was significantly shorter than experiment by 7% and the bulk modulus overestimated experiment by 58%. Calculations on the atomic electronic structure (i.e., isolated atoms and molecules, not a solid) were also performed and the results were very sensitive to the level of correlation included in the calculation. Crocombette et al. also under predicted the experimental lattice constant [9] of bcc uranium by approximately 3%.

Taylor [7] investigated pure systems of uranium using a projector augmented-wave (PAW) pseudopotential utilizing the Perdew–Wang 91 [10] (PW91) Generalized Gradient

---

* Corresponding author.
*E-mail address:* benbeeler@gatech.edu (B. Beeler).

0022-3115/$ - see front matter © 2012 Elsevier B.V. All rights reserved.
http://dx.doi.org/10.1016/j.jnucmat.2012.09.019

**Table 1**
Brief summary of previous computational work investigating properties of U with a reference to an historical review covering experimental work in U.

| Author | Year | Reference | Methodology | Summary |
|---|---|---|---|---|
| Lander et al. | 1994 | [17] | Experimental | Historical review of α U properties |
| Eriksson et al. | 1993 | [3] | Full potential linear muffin-tin orbital | Investigation of crystal structure of α U and f orbital occupation |
| Crocombette et al. | 2001 | [8] | Norm-conserving Pseudopotentials | Crystal structure, cohesive energy and bulk modulus of α, γ and fcc U |
| Taylor | 2008 | [7] | PAW Pseudopotential (PW91 GGA) | Crystal structure and elastic constants of α, γ and fcc U, vacancy formation energy in α U and (001) surface properties |
| Xiang et al. | 2008 | [12] | PAW Pseudopotential (PBE GGA) | Crystal structure and DOS of α, γ and bct U, vacancy formation energy in γ U, Nb point defects |
| Shang et al. | 2010 | [11] | PAW Pseudopotential (PW91 GGA) | Lattice constants and elastic constants of γ, fcc and hcp U |
| Li et al. | 2012 | [14] | Pseudopotential (PW91 GGA) | Crystal structure, energy and elastic constants of α, β, γ, fcc and hcp U |

Approximation (GGA) of the exchange–correlation functional. Taylor investigated α, γ and face-centered cubic uranium, calculating the equilibrium lattice parameters and the elastic constants of the three structures. The lattice constants of α uranium were predicted within 1% compared to the experimental values (determined at 50 K) [6]. The lattice constant of the bcc structure was slightly lower than the experimental lattice constant at 298 K by approximately 1%. The lattice constant of face-centered cubic (fcc) uranium was analyzed and compared with the results of Crocombette. Taylor predicted an equilibrium lattice constant for fcc uranium that is 4% larger than predicted by Crocombette.

Shang et al. [11] recently performed a comprehensive analysis of the bcc, fcc, and hcp crystal structures investigating uranium as well as the majority of the periodic table. Properties calculated include the optimized lattice constant, the bulk modulus and the elastic constants. Shang et al. used the PW91 GGA for their calculations. Although Shang and Taylor used the same implementation of the exchange–correlation functional, their results for the elastic constants in the bcc phase and the fcc structure showed great variance.

Xiang et al. [12] calculated the equilibrium volumes of the α and γ phases. Also, Xiang calculated the equilibrium volume of a body-centered tetragonal (bct) structure as an approximation of the β phase. Xiang utilized the Perdew–Burke–Ernzerhof (PBE) [13] GGA of the exchange–correlation functional, but this investigation was limited to only equilibrium volumes of three structures, and a calculation of the bulk modulus in the α and γ phases. Utilizing the PBE exchange–correlation functional should yield results slightly variant from those calculated using the PW91 implementation; this is seen in the calculations by Xiang.

Li et al. [14] calculated the energy per atom, structure, and elastic constants of alpha, beta and gamma uranium, along with fcc, hcp and bct U structures utilizing the PW91 GGA. Three structures were evaluated and the lowest structure determined was found to be in agreement with the neutron diffraction experiments from Lawson et al. [1] with regards to determination of the proper crystal structure of the β phase.

Investigations on the phase stability of uranium have been conducted by Soderlind et al. [15] and Adak et al. [16]. Using self-consistent *ab initio* lattice dynamics, Soderlind et al. [15] calculated phonon density of states to investigate instability of the γ phase at 0 K and to show that at high temperatures, the bcc structure (γ phase) is promoted. Adak et al. [16] investigated the high pressure behavior of uranium up to 1.3 TPa. It was shown that the α phase transforms into a bct structure above approximately 285 GPa. At high pressures, the bcc structure (γ phase) of U is energetically favorable when compared to the bct structure. A summary of previous computational investigations of U is presented in Table 1.

Historically, the PW91 and PBE GGA exchange correlation functionals have been regarded as essentially equivalent. Results on simple test systems analyzing lattice constants and cohesive energies yield virtually identical results. However, investigations into the PW91 GGA and the PBE GGA of the exchange correlation functional have shown significant differences in a variety of simulations [18]. Mattsson et al. [18] have shown that large discrepancies can be seen between the two GGAs for surface calculations and monovacancy formation energies. Thus, a comprehensive study of lattice and elastic properties is warranted using the PBE GGA exchange correlation functional to determine possible discrepancies from the PW91 GGA. The PBE formulation is an update and an improvement over the PW91 formulation [13]. Improvements over PW91 include an accurate description of the linear response of the uniform electron gas, correct behavior under uniform scaling, and a smoother potential [13]. Although there has been investigation into the structure and elastic properties of α and γ uranium utilizing the PW91 GGA, there is no previous work utilizing the PBE GGA for the calculation of elastic properties of any uranium phase.

In this paper, a study of the equilibrium lattice constants and elastic constants in five structures of uranium-α, β, body-centered tetragonal, γ, face-centered cubic- using pseudopotential based density functional theory calculations is performed. The structural and elastic properties are calculated for all three uranium phases as well as for the body-centered tetragonal and face-centered cubic structures. The properties of the α phase are compared with the well-documented results of Söderlind, Taylor, Crocombette and experimental results. The properties of the γ phase are compared with those predicted by Taylor and Shang, as well as with experimental values in the literature. The body-centered tetragonal structure is compared with results from Xiang and Söderlind. The face-centered cubic structure of uranium is compared with previous computational results from Taylor and Crocombette. Finally, the Density of States is calculated for all five crystal structures of interest. This is the first comprehensive investigation into equilibrium properties and elastic constants using the PBE GGA of the exchange–correlation functional. This is also the first computational investigation of any kind into the β phase of uranium utilizing the PBE GGA exchange–correlation functional.

## 2. Computational details

The projector augmented wave (PAW) method [19] is utilized within the density functional theory [20,21] framework in the Vienna *ab initio* Simulation Package (VASP) [22–24]. Calculations are performed using the Perdew–Burke–Ernzerhof (PBE) [13] generalized gradient approximation (GGA) description of the exchange–correlation. Methfessel and Paxton's smearing method [25] of the first order is used with a width of 0.2 eV to determine the partial occupancies for each wave function. Spin polarized relaxations are performed using the conjugate gradient method with a convergence criterion on the magnitude of forces at 0.02 eV/Ang. A uranium PAW pseudopotential with the $6s^26p^65f^36d^17s^2$ valence electronic configuration and a core represented by [Xe, 5d, 4f] is utilized. For the α and γ phases, as well as the bct and fcc structures, a unit cell is analyzed with a gamma-centered *k*-point mesh of 20 × 20 × 20 and all symmetry restrictions removed, resulting in 4004 *k*-points in the irreducible Brillouin zone. For the β phase, calculations are performed on the unit cell with a *k*-points mesh of 3 × 5 × 5, resulting in 23 *k*-points in the irreducible wedge of the Brillouin zone. The standard 500 setting is used, which sets precision to accurate and the cutoff energy to 500 eV. Setting the precision to accurate avoids wrap around errors and creates a finer grid for augmentation charges, charge densities and potentials.

For the structural relaxation to calculate equilibrium lattice constants, dynamic boundary conditions are employed, allowing cell volume and cell shape to change, along with the relaxation of atom positions. For the calculation of elastic constants, the elastic tensor is determined by performing finite distortions of the lattice and deriving the elastic constants from the strain–stress relationship [26]. The elastic tensor is calculated both, for rigid ions, as well as allowing for internal relaxation of the ions. The ionic contributions are determined by inverting the ionic Hessian matrix and multiplying with the internal strain tensor [27]. The final elastic moduli including both, the contributions for distortions with rigid ions and the contributions from the ionic relaxations, are reported here.

In order to compute polycrystalline elastic moduli, we apply the Voigt–Reuss–Hill approximation [28]. In this approach, the actual effective modulus for a polycrystalline system is approximated by the arithmetic mean of the two well-known bounds for monocrystals according to Voigt [29] and Reuss and Agnew [30]. The polycrystalline mechanical properties calculated here include the bulk modulus ($B$), shear modulus ($G$), Young's modulus ($E$), Poisson's ratio ($\sigma$) and the Debye temperature ($\theta_D$) [31]. The mathematical formulation is provided in the following equations:

$$B = \frac{1}{9}(c_{11} + c_{22} + c_{33} + 2c_{12} + 2c_{13} + 2c_{23}) \tag{1}$$

$$G = \frac{1}{2}\left[\frac{c_{11} - c_{12} - 3c_{44}}{5} + \frac{5c_{44}(c_{11} - c_{12})}{4c_{44} + 3(c_{11} - c_{11})}\right] \tag{2}$$

$$E = \frac{9BG}{3B + G} \tag{3}$$

$$\sigma = \frac{3B - E}{6B} \tag{4}$$

One of the standard methods to calculate $\theta_D$ is from elastic constants data, since $\theta_D$ may be estimated from the average sound velocity, $v_m$, from the following equation [32]:

$$\theta_D = \frac{h}{k_B}\left[\frac{3}{4\pi V_a}\right]^{1/3} v_m \tag{5}$$

where $h$, $k_B$ and $V_a$ are the Planck's constant, Boltzmann's constant and the average atomic volume, respectively. The average sound velocity in the polycrystalline material is given by [33]:

$$v_m = \left[\frac{1}{3}\left(\frac{2}{v_l^3} + \frac{1}{v_l^3}\right)\right]^{-1/3} \tag{6}$$

where $v_t$ and $v_l$ are the transverse and longitudinal sound velocities in an isotropic material. These can be obtained from the density, $\rho$, the shear modulus and the bulk modulus using Navier's equation [32]:

$$v_l = \left(\frac{3B + 4G}{3\rho}\right)^{1/2} \text{ and } v_t = \left(\frac{G}{\rho}\right)^{1/2} \tag{7}$$

### 2.1. Structure and elastic constants of the α phase

The α phase has a face-centered orthorhombic structure with four atoms in the unit cell (A20 *Strukturbericht* designation, Cmcm space group and oC4 Pearson symbol) as shown in Fig. 1. The α phase is the stable phase at temperatures below 935 K [34]. The α phase is of interest to the nuclear fuel community, as it is present on the radial periphery of metallic uranium alloy nuclear fuel pellets [35] and is also present in spent fuel. The condensed matter community also has had interest in α uranium as a superconductor, as pressure induced superconductivity was discovered by Aschermann and Justi [36]. There are also such phenomena as low temperature charge density waves (CDW) transitions [37] that are of interest to the materials and physics communities. The α phase of uranium has been investigated experimentally, as well as through full-potential and pseudopotential computational methods.

The lattice parameters and volume per atom are presented in Table 2. The calculated elastic constants are presented in Table 3.

The calculated lattice constants compare very well to those of Taylor, Söderlind and Barrett. Utilizing the PBE GGA exchange correlation functional instead of the PW91 used by Taylor produces minor changes in the lattice parameters and in the overall volume per atom. These calculations slightly underestimate lattice constants and the volume per atom when compared to experimental results at 50 K.

The elastic constant results presented in Table 3 were used to calculate polycrystalline bulk properties using Eqs. (1)–(7). Contributions to the elastic moduli from internal relaxations are negligible. The polycrystalline properties of α uranium are presented in Table 4. These results are also compared to experimental information from Morss [39].

The primary direction elastic constants ($c_{11}$, $c_{22}$, $c_{33}$) show excellent agreement with one another and overestimate the experimental results in all cases. The relative magnitude of these elastic constants are consistent, with $c_{33}$ the largest and $c_{22}$ the smallest of these three. For $c_{12}$, excellent agreement is seen for all computational strategies with the experimental results. For $c_{13}$, $c_{23}$, $c_{55}$, $c_{66}$, the bulk modulus ($B$), the shear modulus ($G$), and the Debye temperature, this work and that of Taylor slightly overestimate the experimental results. Söderlind's results produce an underestimate in the case of $c_{13}$ and the shear modulus, and yield overestimates for the remaining elastic constants. For $c_{44}$, Taylor's and Söderlind's calculated values are an overestimate, whereas this work calculates an underestimate of the experimental value. A

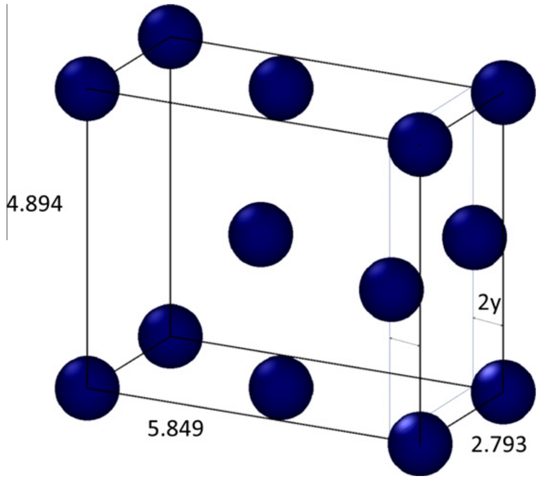

**Fig. 1.** The α uranium unit cell. Dimensions are in Å. Calculated values of lattice parameters are shown in Table 2 along with comparisons with literature.

**Table 2**
The optimized lattice constants (Å), internal parameters and volume per atom (Å$^3$) for α uranium. Results are compared with pseudopotential calculations from Taylor (PW91) [7], full-potential (FP) calculations from Söderlind [4], norm-conserving (NC) pseudopotential calculations from Crocombette [8] and experimental (expt) work at 50 K from Barrett [6]. The internal parameter y is unitless. Fig. 1 shows the unit cell for α-U.

| | This work (PBE) | Taylor (PW91) | Söderlind (FP) | Crocombette (NC) | Barrett (expt) |
|---|---|---|---|---|---|
| $A$ | 2.793 | 2.800 | 2.845 | 2.809 | 2.836 |
| $B$ | 5.849 | 5.896 | 5.818 | 5.447 | 5.867 |
| $C$ | 4.894 | 4.893 | 4.996 | 4.964 | 4.936 |
| $Y$ | 0.098 | 0.097 | 0.103 | – | 0.102 |
| Volume/atom | 19.987 | 20.194 | 20.674 | 19.026 | 20.535 |

**Table 3**
Elastic constants of αU. Results are compared with pseudopotential calculations from Taylor [7], full-potential calculations from Söderlind [4] and experiments at 298 K from Fisher and McSkimin [38]. Elastic constants are given in GPa.

| | This work (PBE) | Taylor (PW91) | Söderlind (FP) | Fisher (expt) |
|---|---|---|---|---|
| $C_{11}$ | 299 | 296 | 300 | 215 |
| $C_{22}$ | 231 | 216 | 220 | 199 |
| $C_{33}$ | 364 | 367 | 320 | 267 |
| $C_{12}$ | 59 | 60 | 50 | 46 |
| $C_{13}$ | 30 | 29 | 5 | 22 |
| $C_{23}$ | 144 | 141 | 110 | 108 |
| $C_{44}$ | 100 | 153 | 150 | 124 |
| $C_{55}$ | 150 | 129 | 93 | 73 |
| $C_{66}$ | 132 | 99 | 120 | 74 |

comparison between GGA exchange correlation functionals shows that the largest variance occurs in the elastic constants based upon shear distortions ($c_{44}$, $c_{55}$, $c_{66}$).

### 2.2. Structure and elastic constants of the β phase

There was controversy [40] over the structure of the β phase of uranium until 1988, when Lawson published neutron powder diffraction experiments [1]. A discussion of this controversy is beyond the scope of this paper, but was summarized by Donohue and Einspahr [40]. The β phase of uranium has a tetragonal structure with 30 atoms in the unit cell (D8$_b$ *Strukturbericht* designation, P4$_2$/mnm space group and the tP30 Pearson's symbol) as shown in Fig. 2. Experimental investigation of the β phase of uranium is difficult due to the small temperature range of stability (935–1045 K) and low pressure range of stability ($P < 3$ GPa) [34]. It is also extraordinarily difficult to grow single crystals of pure β uranium. Single crystals of β uranium can be prepared and quenched to room temperature, and such crystals have been stabilized using small concentrations of chromium, but it is not known whether these alloys have the same structure as the β phase [1].

The lattice constants and volume per atom of β uranium are presented in Table 5 and compared with experimental results calculated at 955 K and computational results from Li [14]. The calculated volume per atom is 5.9% less than experiment, and only a slight deviation in the $a/c$ ratio; 1.9 experimentally, 1.85 calculated. These calculations using DFT were inherently performed at 0 K, and thus we would expect an underestimation of lattice constants when compared to experimental results at 955 K. This work shows an equilibrium structure that is slightly smaller than that predicted by Li, but almost equivalent $a/c$ ratios.

Due to the complexity of the β phase, a body-centered tetragonal (bct) structure is often analyzed instead [12,34]. Also, it has been suggested that an α to bct phase transition occurs at high pressures, but at less than 100 GPa [5,41]. The bct structure has 2 atoms per unit cell, and is thus much less computationally expensive to investigate than the 30 atom unit cell of β uranium. A unit cell of β uranium is shown in Fig. 3 with two parallelepipeds outlined and atoms contained inside the parallelepipeds are darkened (dimensions are given in Å). The two parallelepipeds constitute a repeating structure in β uranium. This set of two parallelepipeds is close to tetragonal (5.894, 5.634, 4.663), but far from body centered. The atoms in the center of this two-parallelepiped system are configured as a tetrahedron. Also, one of the parallelepipeds has two face-centered atoms. Thus, although the bct structure has been used as a simplification of the β phase of uranium, there is a large amount of variance between the two structures and β uranium cannot directly reduce to a bct structure.

An analysis of the energy per atom of the β phase and the bct structure shows that the energy of β phase is slightly lower ($E_\beta = -11.1867$ eV/atom, $E_{\text{bct}} = -11.1489$ eV/atom). Thus, the β phase is more energetically favorable than the bct. The equilibrium lattice parameters and volume per atom of bct uranium are presented in Table 6 and compared with previous calculations by Xiang et al. [12], Soderlind [34] and Li et al., [14]. The volume per atom compares favorably with Xiang [12], however, Xiang does not provide lattice constants. Söderlind [34] calculated the $c/a$ ratio of lattice constants to be 0.82, which compares very favorably with our calculated value of 0.8. Li et al. [14] calculated the lattice constants of the bct structure for U using PAW pseudopotentials. The value of $a$ compares very favorably with the results from this work. However, the calculated value of c from Li is vastly different from the results in this work, and what would be expected from the results of Xiang, and the reported $c/a$ ratio from Soderlind [34].

The elastic constants for β uranium and bct uranium were calculated by performing finite distortions of the lattice and deriving the elastic constants from the strain–stress relationship [26]. These elastic constants are presented in Table 7. Inclusion of internal relaxations in the calculation of the elastic constants significantly impacts the magnitude of the total elastic moduli. For $c_{11}$, $c_{12}$ and $c_{13}$, internal relaxations have a negligible impact. However, for $c_{33}$, $c_{44}$ and $c_{55}$, internal relaxations represent 20%, 15% and 32%, respectively, of the total elastic moduli. Eqs. (1)–(7) were used

**Table 4**
Polycrystalline properties of α uranium calculated from elastic constants. The bulk modulus, $B$, shear modulus, $G$, Young's modulus, $E$, Poisson's ratio, $\sigma$, and the Debye temperature, $\theta_D$ are calculated for this work and compared to Taylor [7], Söderlind [4], Fisher and McSkimin [38] and Morss et al. [39].

| | This work (PBE) | Taylor (PW91) | Söderlind (FP) | Fisher (expt) | Morss (expt) |
|---|---|---|---|---|---|
| $B$ (GPa) | 151 | 149 | 130 | 115 | 100 |
| $G$ (GPa) | 111 | 108 | 68 | 87 | 111 |
| $E$ (GPa) | 267 | 261 | 247 | 206 | 208 |
| $\sigma$ | 0.21 | 0.21 | 0.18 | 0.2 | 0.23 |
| $\theta_D$ (K) | 287 | 287 | 228 | 251 | – |

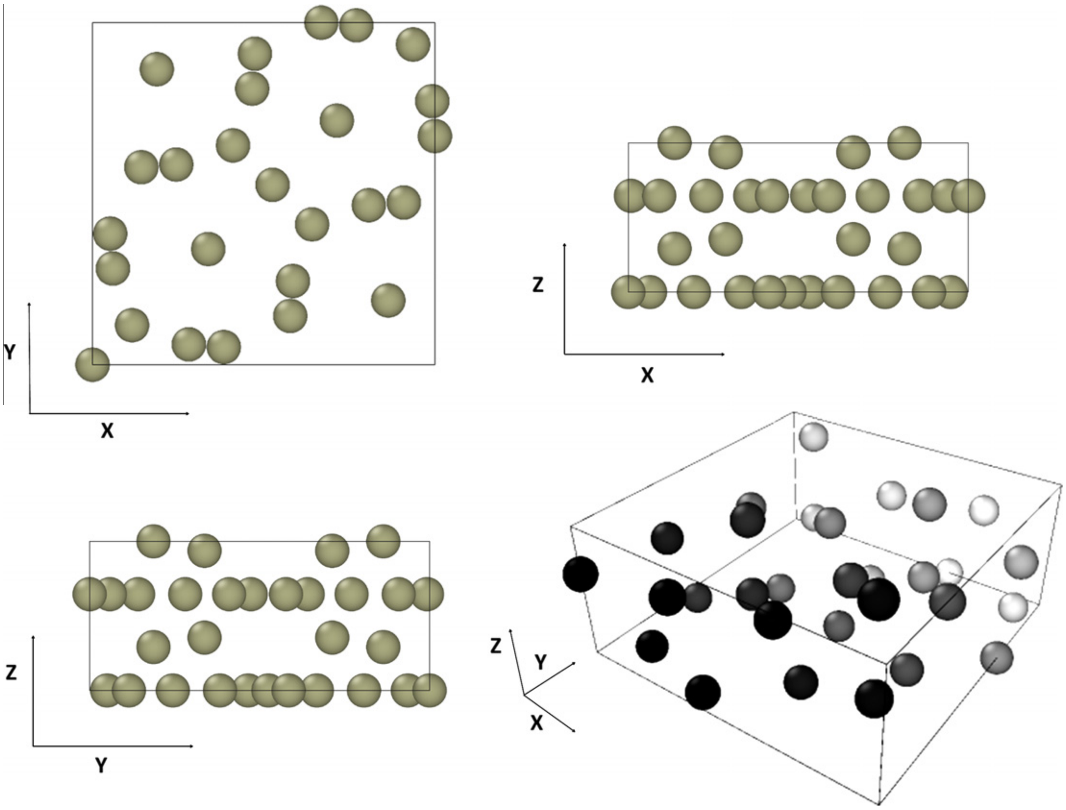

**Fig. 2.** The β uranium unit cell.

**Table 5**
The optimized lattice constants (Å) and volume per atom ($Å^3$) for β uranium. Results are compared with computational work from Li et al. [14] and experimental work from Lawson et al. [1].

| | This work | Li | Expt. (955 K) |
|---|---|---|---|
| *a* | 10.454 | 10.520 | 10.759 |
| *c* | 5.634 | 5.707 | 5.653 |
| Volume/atom | 20.524 | 21.053 | 21.812 |

**Table 6**
Optimized lattice constants (Å) and volume per atom ($Å^3$) of body-centered tetragonal uranium. The calculated volume per atom is compared to the result of Xiang et al. [12], Soderlind [34] and Li et al. [14].

| | This work | Xiang | Soderlind | Li |
|---|---|---|---|---|
| *a* | 3.695 | – | – | 3.72 |
| *c*/*a* | 0.8 | – | 0.82 | 1.24 |
| Volume/atom | 20.268 | 20.5 | – | 31.896 |

to calculated bulk polycrystalline properties. In comparison with work by Li et al. [14], the elastic constants of β U utilizing the PBE GGA compare very favorably to results using the PW91 GGA. However, there is a large discrepancy for the $C_{55}$ elastic constant. For the bct U structure, the $C_{11}$ and $C_{33}$ elastic constants are significantly larger than those calculated by Li. Also, substantial variance is shown for the $C_{44}$ and $C_{55}$ elastic constants. Thus, for the β phase or U and the bct structure of U, the PBE and PW91 GGA exchange–correlation functionals show a general agreement, but significant

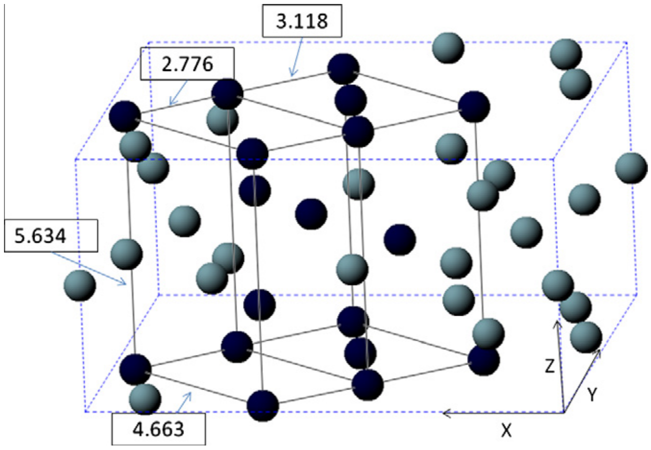

**Fig. 3.** The β phase of uranium, with an attempted approximation to a body-centered tetragonal crystal structure. The two parallelepipeds outlined in the unit cell constitute a repeating structure in β uranium, but are not bct. The dimensions of the parallelepiped are given in Å.

**Table 7**
Elastic properties of the β phase of uranium and the body-centered tetragonal structure of uranium. The Debye temperature is given in units of degrees K, the Poisson's ratio is unitless and the elastic constants and polycrystalline elastic moduli are given in GPa. Results from this worked are compared with the of Li.

| | β-U | β (Li) | bct U | bct (Li) |
|---|---|---|---|---|
| $C_{11}$ | 220 | 218 | 264 | 230 |
| $C_{33}$ | 201 | 214 | 254 | 204 |
| $C_{12}$ | 107 | 99 | 55 | 61 |
| $C_{13}$ | 79 | 80 | 68 | 61 |
| $C_{44}$ | 65 | 60 | 56 | 79 |
| $C_{55}$ | 36 | 61 | 56 | 39 |
| $B$ | 130 | 130 | 129 | 114 |
| $G$ | 85 | – | 102 | – |
| $E$ | 210 | – | 242 | – |
| $\sigma$ | 0.23 | – | 0.19 | – |
| $\theta_D$ | 253 | – | 275 | – |

**Table 8**
The optimized lattice constant (Å) and volume per atom (Å$^3$) of $\gamma$ uranium. Results are compared with PAW pseudopotential calculations of Taylor [7], norm-conserving pseudopotential calculations of Crocombette et al. [8], full-potential calculations of Söderlind [4] and an experiment from Wilson at 298 K [9].

| | This work (PBE) | Taylor (PW91) | Söderlind (FP) | Crocombette (NC) | Wilson (expt) |
|---|---|---|---|---|---|
| $a$ | 3.427 | 3.43 | 3.46 | 3.37 | 3.47 |
| Volume/atom | 20.124 | 20.18 | 20.71 | 19.14 | 20.89 |

discrepancies occur in the calculation of elastic constants. In comparing with α uranium, the polycrystalline properties are generally slightly less in β uranium, than in α uranium. For $B$, $G$, $E$, and $\theta_D$, there is a decrease from α to β from as little as 12% ($\theta_D$) up to 23% ($G$). The Poisson's ratio is approximately equal, but slightly larger in β uranium than in α uranium. For bct uranium, the calculated bulk modulus and Debye temperature are also very similar to that of α and $\gamma$ uranium. In comparing elastic constants of bct uranium to β uranium, there is relatively good agreement. The $c_{11}$ and $c_{33}$ elastic constants are slightly overestimated, whereas the $c_{12}$ and $c_{13}$ elastic constants are slightly underestimated. The result for the bulk modulus is nearly identical. These calculations show that $c_{12}$ is less than $c_{11}$, leading to a positive shear constant; $c' = (c_{11} - c_{12})/2$ and $(c_{11} + c_{33})/2 > c_{13}$, implying stability of both the β phase and the bct structure at 0 K. Thus, even though bct uranium is not a good crystallographic approximation of the β phase of uranium, it can serve as a reasonable approximation for some elastic properties.

### 2.3. Structure and elastic constants of the $\gamma$ phase

The $\gamma$ phase has a body-centered cubic structure with two atoms in the unit cell (A2 *Strukturbericht* designation). The $\gamma$ phase is the stable phase at temperatures from 1045 K to the melting point of 1406 K [34]. The $\gamma$ phase of uranium is of primary interest to the nuclear fuels community. Uranium is often alloyed with Zr or Nb to stabilize the $\gamma$ phase to lower temperatures. This enables the operation of nuclear fuel in a cubic phase, yielding isotropic polycrystalline properties. Experimental investigation of the $\gamma$ phase of uranium is quite difficult due to the low temperature mechanical instability of the crystal structure. This behavior is similar to other metals with a high temperature bcc phase and a ground state face-centered/hexagonal type structure, such as Ti, Zr, and Hf [42]. Quenching the $\gamma$ phase of uranium to low temperatures often results in the $\gamma$ phase decomposing into the α phase. Thus, experiments need to be performed at high temperatures, and this requirement has limited the experimental investigation into the $\gamma$ phase. The lattice parameters and volume per atom are presented in Table 8 and the elastic constants are presented in Table 9. Contributions to the elastic moduli from internal relaxations are negligible.

Using Eqs. (1)–(7), the polycrystalline properties of $\gamma$ uranium are calculated and are presented in Table 10. These results are also compared to an experimental result from Yoo et al. [43]. Using Taylor's [7] elastic constants, the value for the shear modulus ($G$) is negative, leading to unrealistic values for the polycrystalline properties. Thus, the values for the remaining polycrystalline properties are not shown.

**Table 9**
Elastic constants of $\gamma$ uranium. The elastic constants have been calculated and are compared with pseudopotential calculations from Taylor [7] and Shang et al., [11]. Units are GPa.

| | This work (PBE) | Taylor (PW91) | Shang (PW91) |
|---|---|---|---|
| $C_{11}$ | 86 | 161 | 84 |
| $C_{12}$ | 155 | 184 | 159 |
| $C_{44}$ | 37 | 56 | 38 |

**Table 10**
Polycrystalline properties of $\gamma$ uranium calculated from elastic constants in Table 9. The bulk modulus ($B$), shear modulus ($G$), Young's modulus ($E$), Poisson's ratio ($\sigma$) and the Debye temperature ($\theta_D$) are calculated for this work and compared to Taylor [7], Shang et al. [11] and with an experimental bulk modulus from Yoo et al. [43].

| | This work (PBE) | Taylor (PW91) | Shang (PW91) | Yoo (expt) |
|---|---|---|---|---|
| $B$ (GPa) | 132 | 176 | 133 | 113 |
| $G$ (GPa) | 113 | – | 102 | – |
| $E$ (GPa) | 265 | – | 243 | – |
| $\sigma$ | 0.17 | – | 0.20 | – |
| $\theta_D$ (K) | 289 | – | 274 | – |

The elastic constants are compared with pseudopotential calculations from Taylor and Shang who utilized the PW91 GGA exchange–correlation functional. This work compares very favorably to that of Shang but varies quite strongly from Taylor. However, all three calculations show that $c_{12}$ is larger than $c_{11}$, leading to a negative shear constant; $c' = (c_{11} - c_{12})/2$. A negative value for the shear constant predicts mechanical instability at the simulation temperature of 0 K. This is in agreement with previous calculations [34]. The Debye temperature in $\gamma$ uranium is approximately the same as the calculated Debye temperature in α uranium. The only experimental value for comparison is the bulk modulus, determined by Yoo through the fitting of a temperature independent equation of state [43]. This work slightly overestimates the value of the bulk modulus calculated experimentally by Yoo et al. [43].

**Table 11**
Optimized lattice constant (Å) and volume per atom (Å$^3$) of face-centered cubic uranium. Results are compared with previous PAW pseudopotential work from Taylor [7] and norm-conserving pseudopotential work from Crocombette et al. [8].

| | This work (PBE) | Taylor (PW91) | Crocombette (NC) |
|---|---|---|---|
| $a$ | 4.433 | 4.48 | 4.30 |
| Volume/atom | 21.774 | 22.48 | 19.88 |

**Table 12**
Elastic constants of face-centered cubic U. Results are compared with PAW pseudopotential calculations of Taylor [7] and Shang et al. [11]. Units are GPa.

| | This work (PBE) | Taylor (PW91) | Shang (PW91) |
|---|---|---|---|
| $C_{11}$ | 46 | 184 | 14 |
| $C_{12}$ | 144 | 267 | 166 |
| $C_{44}$ | 40 | 28 | 20 |

**Table 13**
Polycrystalline properties of face-centered cubic uranium. The bulk modulus ($B$), shear modulus ($G$), Young's modulus $\epsilon$, Poisson's ratio ($\sigma$) and the Debye temperature ($\theta_D$) are calculated for this work and compared to Taylor [7] and Shang et al. [11].

| | This work (PBE) | Taylor (PW91) | Shang (PW91) |
|---|---|---|---|
| $B$ (GPa) | 111 | 239 | 114 |
| $G$ (GPa) | 76 | 43 | 11 |
| $E$ (GPa) | 185 | 120 | 32 |
| $\sigma$ | 0.22 | 0.42 | 0.45 |
| $\theta_D$ (K) | 241 | 187 | 95 |

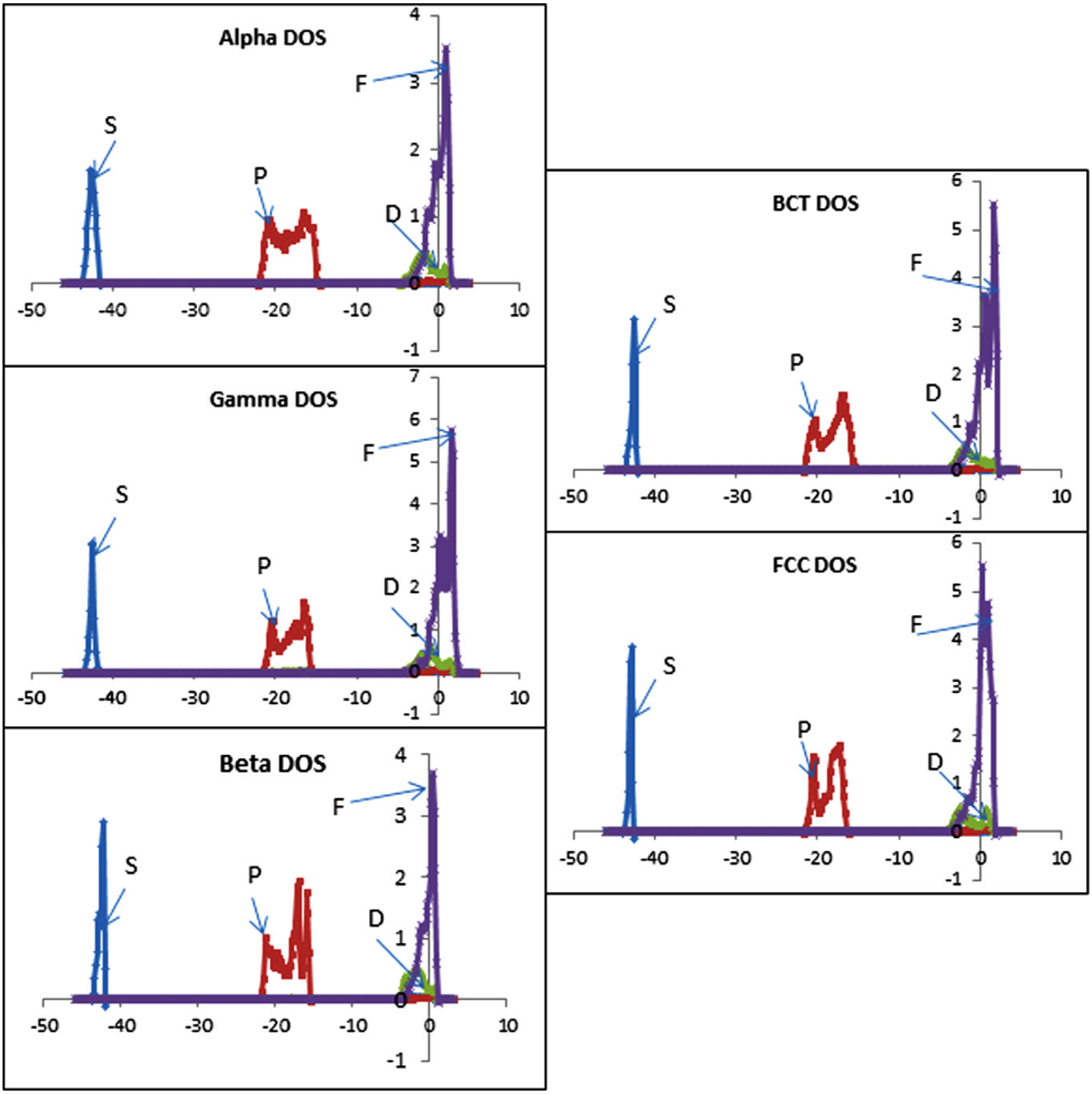

**Fig. 4.** Partial density of states of the α, β and γ phases as well as the bct and fcc structures of U. The 6s, 7s, 6p, 6d and 5f electronic orbitals are included.

### 2.4. Structure and elastic constants of face-centered cubic uranium

The face-centered cubic (fcc) structure (A1 *Strukturbericht* designation) was analyzed for uranium. The fcc structure does not exist on the phase diagram of uranium, but is often analyzed. An approximation of the α phase is the fcc structure, and also, the fcc crystal structure is a very common lattice type and insight can be gained from analyzing lattice and elastic constants of fcc uranium. The lattice parameters and volume per atom are presented in Table 11; the elastic constants are presented in Table 12 and the polycrystalline properties in Table 13. Contributions to the elastic moduli from internal relaxations are negligible.

The lattice constants of fcc uranium compare very favorably to work performed by Taylor [7], with a variance of 1%. The bulk elastic constants of fcc uranium vary quite strongly from those calculated by Taylor. However, a much closer correlation is seen with the calculations by Shang. Excellent agreement is seen in comparing the bulk modulus, and the ratios of lattice constants are similar, with $c_{12}$ being much greater than $c_{11}$ and $c_{44}$. However, the magnitudes of $c_{11}$ and $c_{44}$ are overestimated when compared to Shang, and the magnitude of $c_{12}$ is underestimated.

## 3. Density of states

The density of states (DOS) has been determined in order to analyze variances in electronic structure between the α, β and γ phases as well as the bct and fcc structures. In Fig. 4, the partial density of states are displayed for all five crystal structures with equilibrium lattice constants. The electronic orbitals displayed include 6s, 7s, 6p, 6d and 5f. For all structures analyzed, the s orbitals

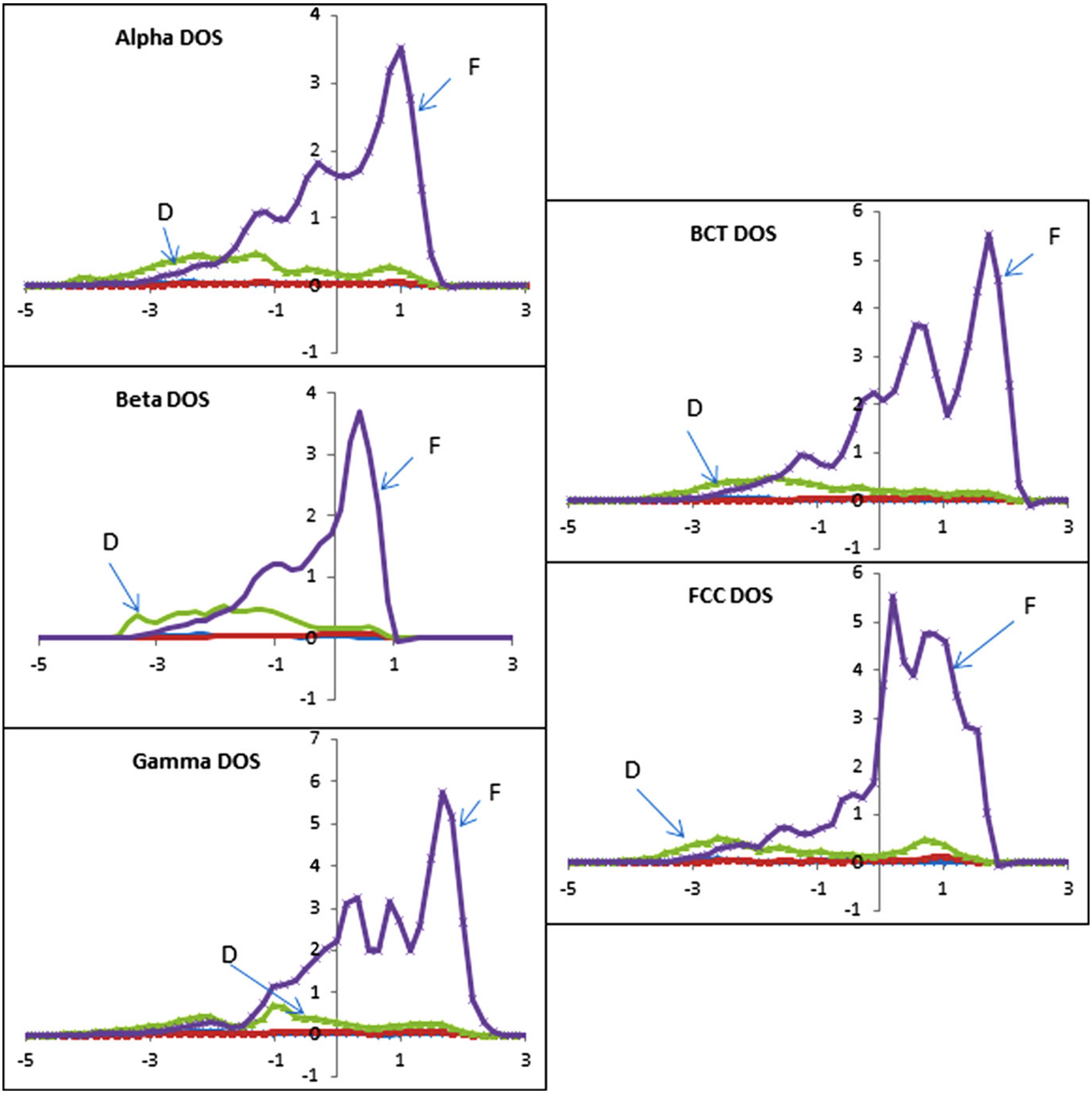

**Fig. 5.** Partial density of states of the α, β and γ phases as well as the bct and fcc structures of U near the Fermi level. The 6d and 5f electronic orbitals are included.

and p orbitals are relatively deep in the core. Near the Fermi level, the f orbital dominates electronic interactions. Although general trends are observed over all structures, minor changes are seen in the core p states. Thus, under high pressure conditions where *p* orbital electrons can potentially be involved in electronic interactions, vastly different bonding behavior is to be expected between the five different structures.

Under equilibrium conditions, typically only electrons at or near the Fermi level will participate in bonding. The partial density of states near the Fermi level for all five structures is displayed in Fig. 5. It can be seen that *f* occupation displays significant variance as a function of crystal structure. Similar behavior is shown for *f* orbital occupation for the α, β and γ phases as well as the bct structure, in that there is gradual increase in *f* occupation as a function of energy around the Fermi level. The fcc partial density of states shows a dramatic increase in *f* occupation directly at the Fermi energy. It is interesting to note that the transition from the α phase to the β phase results in a decrease in the *f* electrons above the Fermi level. However, transitioning from the β phase to the γ phase shows marked increase in the density of *f* electrons above the Fermi level. For the similar crystal structures of bcc (γ phase) and bct U, minimal changes in the partial density of states are shown. For all crystal structures displayed in Fig. 7, 6d electrons exhibit very low densities above the Fermi level, and thus would not be expected to play a major role in bonding.

## 4. Discussion and conclusions

The metallic alloys of uranium are of interest from the perspective of use in a nuclear reactor, especially a fast reactor. Here the γ phase is preferred for its cubic polycrystalline properties. Yet, in the reactor, fission, radiation damage and thermal gradients may precipitate the formation of the β and α phases as well [35,44]. Our calculations show that at 0 K the volume per atom from the α phase to the β phase varies by 2.7% and from the β phase to the γ phase by 1.9%. Also, elastic constants of the α and β phases are anisotropic compared to the isotropic γ phase. Thus, such phase changes would be accompanied by significant lattice strains across phase interfaces. Further investigation needs to be accompanied by experimental observation of phase boundaries and interfaces.

This study analyzed structural and elastic properties of five uranium crystal structures: the face centered orthorhombic A20 structure (α phase), the tetragonal $D8_b$ structure (β phase), body centered tetragonal, body centered cubic (γ phase) and face centered cubic structures. Calculations were performed within the density functional theory framework employing Projector Augmented Wave method and the PBE–GGA exchange correlation. This was the first comprehensive study of elastic properties of uranium utilizing the PBE–GGA exchange correlation functional. It was found that using the updated PBE–GGA, significant differences were seen in the shear elastic constants for α uranium when compared to results using the PW91-GGA. For γ uranium, nearly identical results were produced from this work utilizing the PBE and from Shang utilizing the PW91. For fcc uranium, the ratios of the elastic constants were similar for both GGA implementations, but the magnitudes of the individual elastic constants varied greatly. Thus, implementation of the PBE–GGA formulation is critical in the analysis of elastic properties of uranium, particularly in complex structures such as α uranium. The elastic constants were used to compute polycrystalline elastic moduli, Poisson's ratio and Debye temperature for all five structures. Inclusion of internal relaxation into the calculation of elastic constants was negligible for the α and γ phases, as well as for the bct and fcc structures. However, internal relaxation contributions were significant in the calculation of elastic constants in the β phase of uranium.

For α uranium, the calculations of the primary direction elastic constants ($c_{11}, c_{22}, c_{33}$) showed excellent agreement with previous computational studies and overestimated the experimental results in all cases. The relative magnitude of these elastic constants were consistent, with $c_{33}$ the largest and $c_{22}$ the smallest of these three. A comparison between GGA exchange correlation functionals showed that the largest variance occurred in the elastic constants based upon shear distortions ($c_{44}, c_{55}, c_{66}$), with the largest variance of 53% for $c_{44}$. This was the first theoretical study of the complex tetragonal 30 atom structure of the β phase. In comparing with α uranium, the polycrystalline properties were generally slightly less in β uranium, than in α uranium. In comparing elastic constants of bct uranium to β uranium, there was relatively good agreement. The $c_{11}$ and $c_{33}$ elastic constants were slightly overestimated, whereas the $c_{12}$ and $c_{13}$ elastic constants were slightly underestimated. The bct structure is crystallographically significantly different from the β phase, but exhibits similar elastic properties. For γ uranium, the elastic constants were compared with pseudopotential calculations from Taylor and Shang who utilized the PW91 GGA exchange–correlation functional. This work compared very favorably to that of Shang but varied quite strongly from Taylor. However, Taylor, Shang and this work all predict mechanical instability at the simulation temperature of 0 K. The Debye temperature in γ uranium was approximately the same as the calculated Debye temperature in α uranium. The only experimental value for comparison is the bulk modulus, determined by Yoo through the fitting of a temperature independent equation of state [43]. This work slightly overestimated the value of the bulk modulus calculated experimentally. For fcc uranium, the bulk elastic constants varied quite strongly from those calculated by Taylor. However, a much closer correlation was seen with the calculations by Shang. Excellent agreement was seen in comparing the bulk modulus, and the ratios of lattice constants are similar, with $c_{12}$ being much greater than $c_{11}$ and $c_{44}$. However, the magnitudes of $c_{11}$ and $c_{44}$ were overestimated when compared to Shang, and the magnitude of $c_{12}$ is underestimated. Finally, the density of states was analyzed for the α, β and γ phases of U, as well as the bct and fcc crystal structures. The f orbital electrons are the primary contributors to bonding. The electronic structure around the Fermi energy varies for each crystal structure analyzed. The γ phase is the equilibrium phase with the highest density of f electrons above the Fermi energy. The β phase has the smallest density of f electrons above the Fermi energy.

## Acknowledgements

We acknowledge support from INL subcontract DE-AC07-05ID14517, NRC Faculty Development Grant NRC-38-08-938 and acknowledge computing resources provided by Idaho National Laboratory.

## References

[1] A. Lawson, C. Olsen, J. Richardson, M. Mueller, G. Lander, Acta Cryst. 44B (1988) 89.
[2] J. Akella, S. Weir, J.M. Wills, P. Soderlind, J. Phys.-Condens. Matter 9 (1997) L549–L555.
[3] O. Eriksson, P. Soderlind, J. Willis, A. Boring, Phys. B 190 (1993) 5.
[4] P. Soderlind, Phys. Rev. B 66 (2002) 085113.
[5] P. Soderlind, O. Eriksson, J. Willis, A. Boring, Nature 374 (1995) 524.
[6] C. Barrett, M. Mueller, R. Hitterman, Phys. Rev. B 129 (1963) 625.
[7] C. Taylor, Phys. Rev. B 77 (2008) 094119.
[8] J. Crocombette, F. Jollet, L. Nga, T. Petit, Phys. Rev. B 64 (2001) 104107.
[9] A. Wilson, R. Rundle, Acta Cryst. 2 (1949) 126.
[10] J. Perdew, Y. Wang, Phys. Rev. B 45 (1992) 13244.
[11] S. Shang, A. Saengdeejing, Z. Mei, D. Kim, H. Zhang, S. Ganeshan, Y. Wang, Z. Liu, Comp. Mater. Sci. 48 (2010) 813.
[12] S. Xiang, H. Huang, L. Hsiung, J. Nucl. Mater. 375 (2008) 113.
[13] J. Perdew, K. Burke, M. Ernzerhof, Phys. Rev. Lett. 77 (1996) 3865.
[14] J.H. Li, Q.B. Ren, C.H. Lu, L. Lu, Y. Dai, B.X. Liu, J. Alloys Comp. 516 (2012) 139.
[15] P. Soderlind, B. Grabowski, L. Yang, A. Landa, Phys. Rev. B 85 (2012) 060301.
[16] S. Adak, H. Nakotte, P. de Chatel, B. Kiefer, Phys. B 406 (2011) 3342.
[17] G.H. Lander, E.S. Fisher, S.D. Bader, Adv. Phys. 43 (1994) 1–111.
[18] A. Mattsson, R. Armiento, P. Schultz, T. Mattsson, Phys. Rev. B 73 (2006) 195123.
[19] P. Blochl, O. Jepsen, O. Anderson, Phys. Rev. B 49 (1994) 16223.
[20] P. Hohenberg, W. Kohn, Phys. Rev. 136 (1964) B864.
[21] W. Kohn, L. Sham, Phys. Rev. 140 (1965) A1133.
[22] G. Kresse, J. Furthmuller, Phys. Rev. B 54 (1996) 11169.
[23] G. Kresse, D. Joubert, Phys. Rev. B 59 (1999) 1758.
[24] P. Blochl, Phys. Rev. B 50 (1994) 17953.
[25] M. Methfessel, A. Paxton, Phys. Rev. B 40 (1989) 3616.
[26] Y. Le Page, P. Saxe, Phys. Rev. B 65 (2002) 104104.
[27] X. Wu, D. Vanderbilt, D. Hamann, Phys. Rev. B 72 (2005) 035105.
[28] R. Hill, Proc. Phys. Soc. 65 (1952) 349.
[29] W. Voigt, Lehrbuch der Kristallphysik, Teubner, Leipzig, 1928.
[30] A. Reuss, A. Agnew, Math. Mech. 9 (1929) 49.
[31] M. Ghebouli, B. Ghebouli, M. Fatmi, Phys. B 406 (2011) 1837.
[32] O. Anderson, J. Phys. Chem. Solids 24 (1963) 909.
[33] E. Schreiber, O. Anderson, N. Soga, Elastic Constants and Their Measurements, McGraw-Hill, New York, 1973.
[34] P. Soderlind, Adv. Phys. 47 (1998) 959–998.
[35] G. Hofman, S. Hayes, M. Petri, J. Nucl. Mater. 227 (1996) 277.
[36] G. Aschermann, E. Justi, Phys. Z 43 (1942) 207.
[37] L. Fast, O. Eriksson, B. Johansson, J. Wills, G. Straub, H. Roeder, L. Nordstrom, Phys. Rev. Lett. 81 (1998) 2978.
[38] E. Fisher, H. McSkimin, J. Appl. Phys. 29 (1958) 1473.
[39] L. Morss, N. Edelstein, J. Fuger, The Chemistry of the Actinide and Transactinide Elements, third ed., Springer, Netherlands, 2006.
[40] J. Donohue, H. Einspahr, Acta Crystallographica Section B-Structural Crystallography and Crystal Chemistry B 27 (1971) 1740.
[41] O. Eriksson, J. Willis, P. Soderlind, J. Melsen, R. Ahuja, A. Boring, B. Johansson, J. Alloys Comp. 213 (214) (1994) 268.
[42] J. Sanchez, D. de Fontaine, Phys. Rev. Lett. 35 (1975) 227.
[43] C.S. Yoo, H. Cynn, P. Soderlind, Phys. Rev. B 57 (1998) 10359–10362.
[44] G. Hofman, L. Walter, T. Bauer, Energy 31 (1997) 83.